Soat2 ties cholesterol metabolism to β-oxidation and glucose tolerance in male mice

Camilla Pramfalk, Osman Ahmed, Matteo Pedrelli, Mirko Minniti, Serge Luquet, Raphaël Gp Denis, Maria Olin, Jennifer Härdfeldt, Lise-lotte Vedin, Knut Steffensen, et al.

JIM Original Article

Linked to: S. Romeo J Intern Med 2022; https://doi.org/10.1111/joim.13460. doi: 10.1111/joim.13450

Soat2 ties cholesterol metabolism to β-oxidation and glucose tolerance in male mice

Camilla Pramfalk[1,2], Osman Ahmed[1,3], Matteo Pedrelli[1], Mirko E. Minniti[1], Serge Luquet[4], Raphaël GP Denis[4], Maria Olin[1], Jennifer Härdfeldt[1], Lise-Lotte Vedin[1], Knut R Steffensen[1], Mikael Rydén[2,5], Leanne Hodson[6,7], Mats Eriksson[2,5] & Paolo Parini[1,2]

From the [1]Cardio Metabolic Unit, Department of Medicine and Department of Laboratory Medicine, Karolinska Institutet, Stockholm, Sweden; [2]Medicine Unit Endocrinology, Theme Inflammation and Ageing, Karolinska University Hospital, Stockholm, Sweden; [3]Department of Biochemistry, Faculty of Medicine, Khartoum University, Khartoum, Sudan; [4]Université de Paris, BFA, Paris, France; [5]Unit of Endocrinology, Department of Medicine, Karolinska Institutet at Karolinska University Hospital Huddinge, Stockholm, Sweden; [6]Oxford Centre for Diabetes, Endocrinology and Metabolism, Radcliffe Department of Medicine, University of Oxford, Oxford, UK; and [7]National Institute for Health Research Oxford Biomedical Research Centre, Oxford University Hospital Trusts, Oxford, UK

Abstract. Pramfalk C, Ahmed O, Pedrelli M, Minniti ME, Luquet S, Denis RGP, et al. *Soat2* ties cholesterol metabolism to β-oxidation and glucose tolerance in male mice. *J Intern Med.* 2022;**292:**296–307.

Background. Sterol *O*-acyltransferase 2 (*Soat2)* encodes acyl-coenzyme A:cholesterol acyltransferase 2 (ACAT2*)*, which synthesizes cholesteryl esters in hepatocytes and enterocytes fated either to storage or to secretion into nascent triglyceride-rich lipoproteins.

Objectives. We aimed to unravel the molecular mechanisms leading to reduced hepatic steatosis when *Soat2* is depleted in mice.

Methods. *Soat2*$^{-/-}$ and wild-type mice were fed a high-fat, a high-carbohydrate, or a chow diet, and parameters of lipid and glucose metabolism were assessed.

Results. Glucose, insulin, homeostatic model assessment for insulin resistance (HOMA-IR), oral glucose tolerance (OGTT), and insulin tolerance tests significantly improved in *Soat2*$^{-/-}$ mice, irrespective of the dietary regimes (2-way ANOVA). The significant positive correlations between area under the curve (AUC) OGTT ($r = 0.66$, $p < 0.05$), serum fasting insulin ($r = 0.86$, $p < 0.05$), HOMA-IR ($r = 0.86$, $p < 0.05$), Adipo-IR (0.87, $p < 0.05$), hepatic triglycerides (TGs) ($r = 0.89$, $p < 0.05$), very-low-density lipoprotein (VLDL)-TG ($r = 0.87$, $p < 0.05$) and the hepatic cholesteryl esters in wild-type mice disappeared in *Soat2*$^{-/-}$ mice. Genetic depletion of *Soat2* also increased whole-body oxidation by 30% ($p < 0.05$) compared to wild-type mice.

Conclusion. Our data demonstrate that ACAT2-generated cholesteryl esters negatively affect the metabolic control by retaining TG in the liver and that genetic inhibition of *Soat2* improves liver steatosis via partitioning of lipids into secretory (VLDL-TG) and oxidative (fatty acids) pathways.

Keywords: ACAT2, atherosclerosis, cardiometabolic diseases, cholesteryl esters, CIDEC, GLUT2, insulin resistance, lipoproteins, NAFLD, *Soat2*, triglycerides

Introduction

Disrupted glucose homeostasis by impaired metabolism leads to the inability to maintain normal blood glucose levels, to impaired insulin secretion and to decreased central and peripheral insulin sensitivity. The resulting different clinical conditions are known as cardiometabolic diseases (e.g. atherosclerotic cardiovascular disease), type 2 diabetes mellitus (T2DM), non-alcoholic fatty liver disease (NAFLD), and non-alcoholic steatohepatitis. Dyslipidemia is a common peripheral phenotype of cardiometabolic diseases and typically includes increased plasma levels of triglycerides (TGs), cholesterol remnant, and small dense low-density lipoproteins (LDLs) and reduced high-density lipoproteins (HDLs) [1]. The significant accumulation of TG and cholesteryl esters (CE) inside the hepatocytes

(hepatic steatosis) is another common phenotype of cardiometabolic diseases and is regarded as the hepatic manifestation of the metabolic syndrome.

Hepatocyte nuclear factor (HNF) 1α and 4α play central roles in lipid and carbohydrate metabolism, and mutations in the respective genes cause monogenic forms of T2DM in humans. The first indications for a possible role in carbohydrate metabolism of the cholesterol esterifying enzyme acyl-coenzyme A:cholesterol acyltransferase 2 (ACAT2), which is encoded by the sterol *O*-acyltransferase 2 (*SOAT2*) gene, came when HNF1α [2] and HNF4α [3] were identified as positive regulators of the human *SOAT2* promoter. The finding that heterozygous HNF4α-mutation carriers have lower plasma levels of CE and TG in their very-low-density lipoprotein (VLDL) particles, compared to non-carriers, confirmed the initial pre-clinical studies [3]. The intracellular biosynthesis of CE from unesterified cholesterol (UC) and long-chain fatty acids is carried out by ACAT1 and ACAT2 [4]. ACAT2 is exclusively expressed in normal enterocytes and hepatocytes [5]. ACAT2 is responsible for the synthesis of CE fated to storage and for the formation of the lipid core of chylomicrons and nascent VLDL [6]. In mice, genetic or selective pharmacological inhibition of *Soat2*/ACAT2 protects against atherosclerosis and diet-induced hypercholesterolemia and cholesterol gallstone disease [7–11]. Also, *Soat2*$^{-/-}$ mice are resistant to dietary cholesterol-induced hepatic steatosis [12, 13]. In humans, ACAT2/*SOAT2*—chaperoned by apolipoprotein J—has recently been shown to facilitate the hepatic lipid accumulation following hepatitis C virus infection and nutrient stress [14]. Hence, ACAT2/*SOAT2* increases the risk for NAFLD also after non-obese stress [14].

In previous studies in mice, the effects on glucose metabolism following genetic depletion of *Soat2* were not investigated in detail. Here, we sought to further characterize the role of ACAT2/*Soat2* in glucose and lipid metabolism in male mice fed a high-fat, a high-carbohydrate, or a chow diet.

Material and methods

Animals

Wild-type and *Soat2*$^{-/-}$ mice were generated by heterozygote breeding of mice on an almost pure genetic background (C57BL6, about 95%). Male mice, 9–15 weeks of age, were fed a high-fat diet (HFD; 21% [w/w] fatty acids and 0.05% [w/w] cholesterol) for eight weeks, a high-carbohydrate diet (HCD; 70% [w/w] carbohydrates and <0.05% [w/w] cholesterol) for two-and-a-half weeks, or a chow diet. We studied eight mice per genotype per diet. In an additional experiment, seven-month-old male mice were fed the earlier mentioned HFD for eight weeks. Here, we studied 10 mice per genotype per diet. The studies were approved by the local ethical committee—Stockholm South Ethical Committee, Huddinge, Sweden—and follow the Swedish National Institutes of Health Guide for the Care and Use of Laboratory Animals.

Insulin and oral glucose tolerance tests

After a 4-h fast, mice were intraperitoneally injected with 0.75 U/kg insulin or gavaged with 1 g/kg glucose, and glucose concentrations were monitored up to 120 minutes.

Tissue lipids

Frozen liver sections were stained with Oil red O to visualize lipids. Liver and muscle (soleus and tibialis anterior) lipids were extracted using chloroform:methanol (2:1 v/v) [15]. Samples were analysed using TG, total- and free cholesterol reagents. Esterified cholesterol was calculated by subtracting the free- from total cholesterol and multiplied by 1.67, for use in determining the mass of the fatty acid moiety.

Serum analyses

Serum lipoproteins were separated by size-exclusion chromatography followed by online determination of total cholesterol, UC, and TG [16]. Serum nonesterified fatty acids (NEFAs), insulin, and glucose were assessed by ELISA or colorimetric enzymatic kits.

RNA extraction, cDNA synthesis, and real-time RT-PCR

Total RNA was extracted and transcribed into cDNA, and gene expressions were assessed (primer sequences are available upon request). Fat specific protein 27 (*Fsp27*)/*Cidec* gene expression was also quantified by Taqman. Arbitrary units were calculated by linearization of the C_T values.

Quantification of total lipolytic activities in adipose tissue

Total lipolytic activities in gonadal adipose tissue were assessed using an LPL Activity assay kit

(Roar Biomedical, SIGMA), which is not specific for lipoprotein lipase (LPL), as described in [13].

Western blot

Whole-cell, cytosolic, and membrane proteins were prepared from each individual, and an equal amount of protein from individuals in each group (n = 8 mice/group/genotype) was pooled. Three different protein concentrations were loaded, and proteins were separated by electrophoresis, transferred to nitrocellulose membranes, blocked, and incubated with antibodies against CIDEC, perilipin 2 (PLIN2), and glucose transporter (GLUT) 2 and 4. Bands were visualized and quantified using Odyssey CLx (LI-COR, Lincoln, NE, USA). The slopes of the curves were calculated, and the slopes for wild types of the respective diet were set equal to 1.

Calorimetric analyses

Calorimetric analyses for energy expenditure, O_2 consumption and CO_2 production, respiratory exchange rate, food intake, and spontaneous locomotor activity (beam breaks per hour) were monitored automatically using calorimetric cages as described in [17]. Body composition was measured using EchoMRI (Houston, TX, USA).

Statistics

All data are presented as mean ± SEM unless stated. Data were tested for normality according to the Shapiro–Wilk test. Parameters that were not normally distributed were log-transformed before analysis. Differences were tested using factorial ANOVA with genotype and diet as factors. Differences between the two genotypes fed the same diet were tested using the Student´s t-test. Areas under the curve (AUC) were calculated by the trapezoid method and divided by time. Correlations were performed using Spearman's Rank Correlation. All statistical analyses were performed using Statistica version 12.0 (StatSoft, Tulsa, OK, USA).

Results

Genetic depletion of Soat2 *reduces hepatic steatosis in male mice*

To confirm the role of *Soat2* in hepatic steatosis, we fed male *Soat2*$^{-/-}$ and wild-type mice an HFD for eight weeks, an HCD for two-and-a-half weeks, or a regular chow diet. All diets were low in cholesterol to investigate ACAT2/*Soat2* independent of excess dietary cholesterol, which was instead done by Alger et al. [12, 13]. No significant differences in weight gain during the study were observed between *Soat2*$^{-/-}$ and wild-type mice (Fig. 1a,b). Liver sections stained for lipid droplets showed less intrahepatic lipid accumulation in *Soat2*$^{-/-}$ compared to wild-type mice (Fig. 1c–e). Quantification of these lipids revealed lower levels of hepatic TG ($p < 0.001$; Fig. 1f) and CE ($p < 0.001$; Fig. 1g) in *Soat2*$^{-/-}$ mice. Intrahepatic UC levels did not significantly differ between the two genotypes, independent of the diets. However, the UC levels decreased ($p < 0.01$), were unchanged, or increased ($p < 0.001$) in *Soat2*$^{-/-}$ mice fed HFD, HCD, or chow diet, respectively (Fig. 1h). A strong positive correlation between the hepatic levels of CE and TG was observed in wild-type mice ($r = 0.89$, $p < 0.05$), which disappeared in *Soat2*$^{-/-}$ mice ($r = 0.39$, NS), indicating that the ACAT2-generated CE are an important driving force for TG accumulation in the liver (Table S1).

Increased secretion of TG in VLDL particles was proposed to explain the reduced liver lipid accumulation in male *Soat2*$^{-/-}$ mice when fed a high-cholesterol diet [12]. Increased serum levels of VLDL-TG were reported also in female *Soat2*$^{-/-}$ mice fed low-cholesterol HFD or HCD [13]. In line with these studies, we found male *Soat2*$^{-/-}$ mice to have higher serum levels of total-, VLDL-, and LDL-TG ($p < 0.001$) compared to wild types (Table S2). Interestingly, the hepatic TG levels were strongly and positively correlated with the levels of VLDL-TG in *Soat2*$^{-/-}$ ($r = 0.87$, $p < 0.05$) but not in wild-type ($r = -0.39$, NS) mice, suggesting again that ACAT2-generated CE induce retention of TG in the liver (Table S1). Our results here are in line with previous studies and clearly show that genetic depletion of *Soat2* protects against hepatic steatosis and that this is associated with an increased mobilization of TG from the liver, via increased secretion of TG in VLDL particles [12, 13].

Genetic depletion of Soat2 *improves glucose tolerance in male mice*

In most people, hepatic steatosis results from and promotes insulin resistance, a condition associated with T2DM. Hence, we wanted to investigate the effects of ACAT2 inhibition by genetic depletion of *Soat2* on glucose tolerance, also in light of the role of HNF1α and HNF4α for *SOAT2* gene regulation [2, 3]. Fasting serum glucose ($p < 0.05$) and insulin

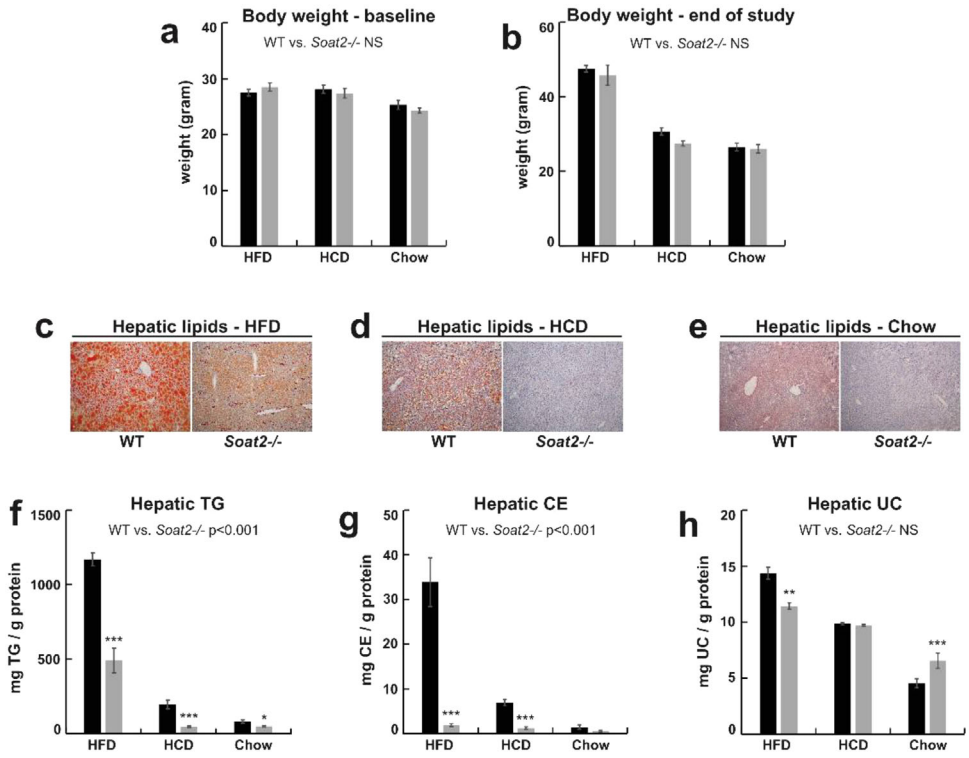

Fig. 1 *Reduced hepatic steatosis in* Soat2$^{-/-}$ *mice. No significant differences in weight-gain were observed between* Soat2$^{-/-}$ *and wild-type (WT) mice (a–b). Frozen liver sections stained with Oil red O (d–e) and quantification of hepatic triglycerides (TG), cholesteryl esters (CE) and unesterified cholesterol (UC) levels (f–h) showed reduced hepatic steatosis in* Soat2$^{-/-}$ *compared to WT mice. Black bars represent WT and grey bars represent* Soat2$^{-/-}$ *mice. Data are expressed as mean ± SEM. Differences were tested using factorial ANOVA with genotype and diet as factors. Differences between the two genotypes fed the same diet were tested using the Student´s* t*-test;* *p < *0.05,* **p < *0.01, and* ***p < *0.001.*

levels ($p < 0.01$), as well as HOMA-IR ($p < 0.01$), were all significantly lower in *Soat2*$^{-/-}$ compared to wild-type mice (Fig. 2a–c, respectively). The effects of *Soat2* genetic depletion were more evident in mice fed HFD. Oral glucose tolerance (OGTT) and insulin tolerance (ITT) tests further supported the evidence of improved glucose tolerance following *Soat2* genetic depletion (AUC OGTT, $p < 0.01$; AUC ITT, $p < 0.001$; Fig. 2d and e and Fig. S1a–f). Again, the effects of *Soat2* genetic depletion were more evident in mice fed HFD.

NEFAs in circulation are the main source of fatty acids for synthesis of TG for secretion in VLDL particles, both in the fasting and postprandial state [18, 19], and insulin suppresses NEFA mobilization from the adipose tissue by inhibition of lipolysis [20]. Since *Soat2*$^{-/-}$ mice had higher serum TG levels and lower serum insulin levels, we were expecting to find higher serum levels of NEFA compared to wild types. Hence, it was a surprise to find that fasting levels in serum of NEFA were not significantly different between *Soat2*$^{-/-}$ and wild-type mice (Fig. 2f). We also found the adipose tissue insulin resistance index (Adipo-IR), calculated by multiplying fasting serum NEFA, to be lower in *Soat2*$^{-/-}$ compared to wild-type mice ($p < 0.01$) (Fig. 2g). Adipose LPL has been shown to become resistant to insulin in diet-induced insulin-resistant rats [21]. Here we found total lipolytic activities in the adipose tissue to be higher in *Soat2*$^{-/-}$ compared to wild-type mice ($p < 0.05$) (Fig. 2h and Fig. S2a–f). Moreover, inverse correlations were observed between total lipolytic activities and Adipo-IR in *Soat2*$^{-/-}$ ($r = -0.60$, $p < 0.05$) and wild-type ($r = -0.77$, $p < 0.05$) mice, suggesting that *Soat2* depletion did not negatively affect insulin signalling in adipose tissue (Table S1).

Intramuscular lipid accumulation has been reported to be associated with dysfunctional insulin sensitivity [22]. Despite the high levels

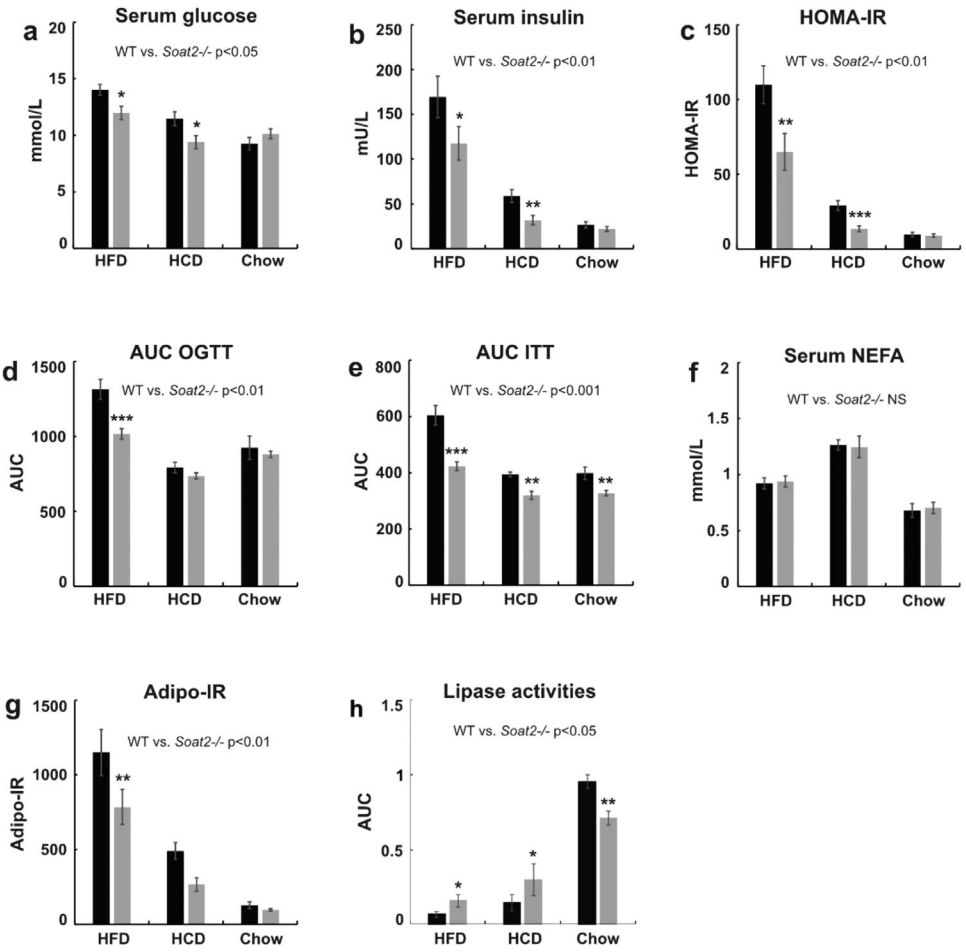

Fig. 2 *Improved glucose tolerance in* Soat2$^{-/-}$ *mice. Glucose, insulin, and HOMA-IR (a–c) together with oral glucose (OGTT) and insulin (ITT) tolerance test (d–e) showed improved glucose tolerance in* Soat2$^{-/-}$ *compared to wild-type (WT) mice. NEFA levels (f) did not significantly differ but the adipose tissue insulin resistance index (Adipo-IR) (g) and assessment of lipase activities in adipose tissue (h) show improved glucose tolerance in* Soat2$^{-/-}$ *mice. Black bars represent WT and grey bars represent* Soat2$^{-/-}$ *mice. Data are expressed as mean ± SEM. Differences were tested using factorial ANOVA with genotype and diet as factors. Differences between the two genotypes fed the same diet were tested using the Student´s* t*-test; *p < 0.05, **p < 0.01 and ***p < 0.001.*

of TG in circulation in *Soat2*$^{-/-}$ mice, quantification of intramuscular lipids revealed less TG accumulation in the Soleus muscle ($p < 0.01$) compared to wild-type mice (Table S3). Further, no significant differences were observed between the two genotypes in intramuscular lipid accumulation (TG and cholesterol) in the tibialis anterior muscle (Table S3). No differences were observed in the protein expression of GLUT4, which mediates insulin-stimulated glucose transport in the muscles, between *Soat2*$^{-/-}$ and wild-type mice (data not shown). Collectively, our data show that genetic depletion of *Soat2* improves both central (hepatic) and peripheral glucose tolerance—an effect that is not associated with the level of TG and NEFA in circulation.

Genetic depletion of Soat2 *decreases hepatic FSP27/CIDEC and GLUT2 expression in male mice*

To investigate more deeply the molecular mechanisms responsible for the diminished hepatic lipid accumulation and improved glucose tolerance following inhibition of ACAT2 by genetic depletion of *Soat2*, key genes involved in hepatic lipid and carbohydrate metabolism were assessed (Table S4).

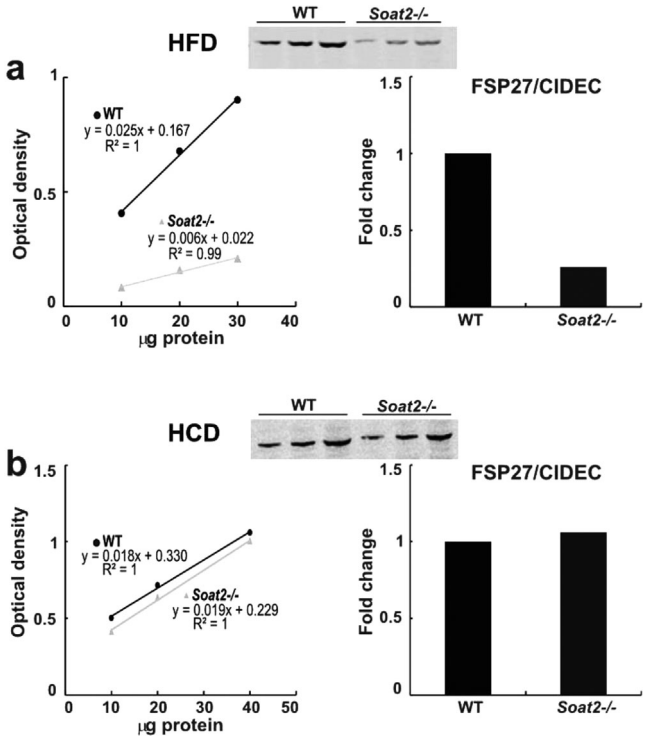

Fig. 3 *Lower hepatic FSP27 protein expression in* Soat2$^{-/-}$ *mice fed a high-fat diet. Whole-cell proteins were prepared from each individual and equal amount of protein from individuals in each group were pooled (*n *= 8 mice/genotype/group). Three different protein concentrations were loaded. The slopes of the curves were calculated and the slopes for wild types (WT) were set equal to 1. The FSP27 protein expressions were more than 50% lower in* Soat2$^{-/-}$ *fed a high-fat diet (a); however, no differences in mice fed a high-carbohydrate diet were observed (b).*

The mRNA expression of acetyl-CoA carboxylase (ACC, encoded by *Acaca*), which catalyses the first and rate-limiting step in *de novo* lipogenesis (DNL), was lower in *Soat2*$^{-/-}$ compared to wild-type mice ($p < 0.001$). The mRNA expression of fat-specific protein 27 (*Fsp27/Cidec*), a lipid droplet (LD) protein known to be upregulated in fatty livers and to enlarge LD [23, 24], was more than 30–60 times higher in wild-type mice fed HFD compared to a chow diet, as expected. Strikingly, the mRNA expression of *Fsp27/Cidec* was dramatically lower in *Soat2*$^{-/-}$ compared to wild-type mice ($p < 0.001$), independent of the diet (Factorial ANOVA, WT vs *Soat2*$^{-/-}$), and this was highly evident in animals fed HFD (98% reduction). Hence, it was not surprising to find that FSP27/CIDEC protein levels were approximately 50% lower in *Soat2*$^{-/-}$ mice fed HFD, whereas no major differences were present between the two genotypes when the mice were fed HCD (Fig. 3a,b). PLIN2 and PLIN3 are two additional LD-associated proteins, and, similar to *Fsp27/Cidec*, we found lower *Plin2* and *Plin3* mRNA levels ($p < 0.001$) in *Soat2*$^{-/-}$ mice. However, this similarity was lost for the hepatic PLIN2 protein expression since no major differences were observed between the two genotypes fed HFD (Fig. S3). Collectively, our data show that genetic depletion of *Soat2* affects the gene expression of important LD-associated proteins and determines lower hepatic FSP27/CIDEC relative to PLIN2 protein expression.

Glucokinase (encoded by *Gck*) catalyses the conversion of glucose into glucose-6-phosphate, and GLUT2 (encoded by *Slc2a2*) is responsible for the bidirectional transport of glucose over the plasma membrane. We found *Gck* mRNA levels ($p < 0.01$) (Table S4) and GLUT2 membrane protein levels (Fig. 4a–d) to be lower in *Soat2*$^{-/-}$ compared to wild-type mice. Thus, the diminished hepatic steatosis and improved glucose tolerance observed in *Soat2*$^{-/-}$ mice involve *Acaca*, *Plin2*, *Plin3*, FSP27/CIDEC, *Gck*, and GLUT2.

Association between hepatic CE levels and parameters of glucose metabolism

In wild-type but not in *Soat2*$^{-/-}$ mice, the hepatic CE levels were positively correlated with the AUC OGTT ($r = 0.66$, $p < 0.05$), serum fasting insulin ($r = 0.86$, $p < 0.05$), HOMA-IR ($r = 0.86$, $p < 0.05$), and Adipo-IR (0.87, $p < 0.05$) levels (Table S1). The hepatic CE levels were positively correlated with serum levels of glucose and AUC ITT in both

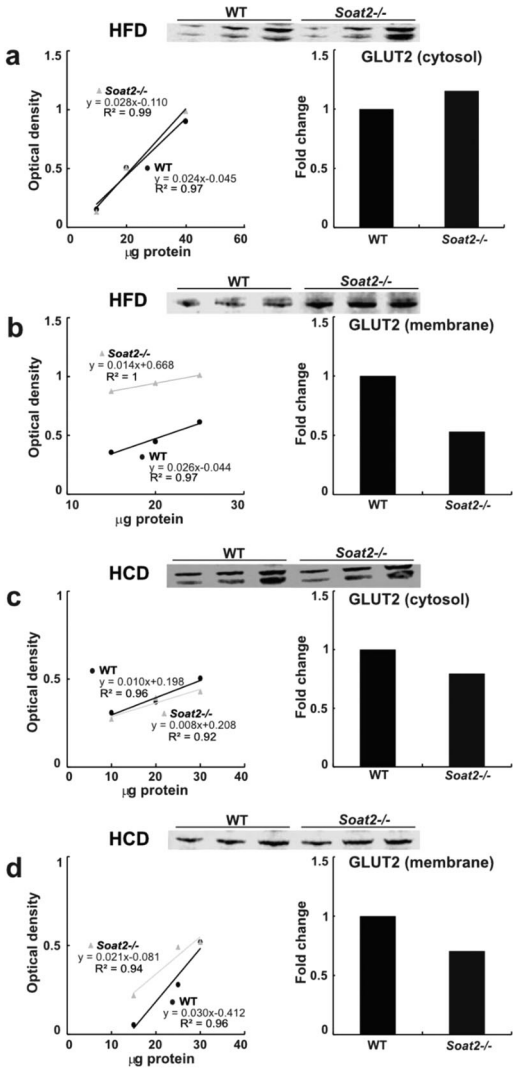

Fig. 4 *Lower hepatic GLUT2 membrane protein expression in* Soat2$^{-/-}$ *mice. Cytosolic and membrane fractions were prepared from each individual and an equal amount of protein from individuals in each group was pooled (*n *= 8 mice/genotype/group). Three different protein concentrations were loaded. The slopes of the curves were calculated and the slopes for wild-type (WT) mice were set equal to 1.* Soat2$^{-/-}$ *mice fed either a high-fat (a and b) or a high-carbohydrate (c and d) diet had lower GLUT2 membrane protein expression compared to WT mice.*

wild-type (0.76 and 0.68, $p < 0.05$) and *Soat2*$^{-/-}$ (0.47 and 0.63, $p < 0.05$) mice, respectively (Table S1). Moreover, hepatic CE levels were inversely correlated with total lipolytic activity in wild-type (−0.75, $p < 0.05$) and *Soat2*$^{-/-}$ (−0.66, $p < 0.05$) mice (Table S1).

Genetic depletion of Soat2 *increases β-oxidation in male mice*

To further understand the consequences of absence of ACAT2 activity due to genetic depletion of *Soat2* onto metabolic efficiency and adult adaptation to an energy-rich diet, approximately seven-month-old *Soat2*$^{-/-}$ mice were fed HFD for eight weeks prior to metabolic characterization. Using automated recording of food, water, locomotor activity, energy expenditure, and respiratory quotient—RER = VCO_2/VO_2 indicative of the substrate being used, RER = 1 for carbohydrate and 0.7 for lipid—we did not find any significant difference in high fat-induced body weight-gain (Fig. 5a), body composition (lean and fat mass), food and water intake, spontaneous locomotor activity, energy expenditure, O_2 consumption and CO_2 production, or respiratory exchange rate (data not shown) between *Soat2*$^{-/-}$ and wild-type mice. In agreement with what we observed in the younger mice, *Soat2*$^{-/-}$ mice had lower hepatic TG ($p < 0.05$) (Fig. 5b) and CE ($p < 0.001$) (Fig. 5c), whereas levels of UC (Fig. 5d) did not significantly differ compared to wild types. Also, serum levels of total-TG ($p < 0.01$) and LDL-TG ($p < 0.001$) were higher in *Soat2*$^{-/-}$ compared to wild-type mice (Table S5). Of fundamental importance was the observation that whole-body oxidation was about 30% higher ($p < 0.05$) in *Soat2*$^{-/-}$ compared to wild-type mice (Fig. 5e,f), indicating a whole-body shift toward lipid-based substrate utilization. Interestingly, analysis of key genes regulating β-oxidation showed a 100% increase in *Ctp1a* mRNA levels in *Soat2*$^{-/-}$ compared to wild-type mice in the tibialis anterior, which was paralleled by around a 10% decrease in genes belonging to the *Acad* family (Fig. S5d).

OGTT, ITT, and fasting serum glucose levels did not significantly differ, while fasting serum levels of insulin were lower ($p < 0.05$), with a similar trend for HOMA-IR, in *Soat2*$^{-/-}$ compared to wild-type mice (Fig. S4a–e). Also, in agreement with what we observed in the younger mice, fasting serum levels of NEFA did not differ but Adipo-IR was lower ($p < 0.05$) in *Soat2*$^{-/-}$ compared to wild-type mice (Fig. S4f,g). Hence, although genetic depletion of *Soat2* seems to have a lesser impact on parameters of glucose tolerance in older mice, less insulin is needed to maintain glucose homeostasis in *Soat2*$^{-/-}$ compared to wild-type mice also when ageing, indicative of a certain degree of resilience against diet-induced diabetes.

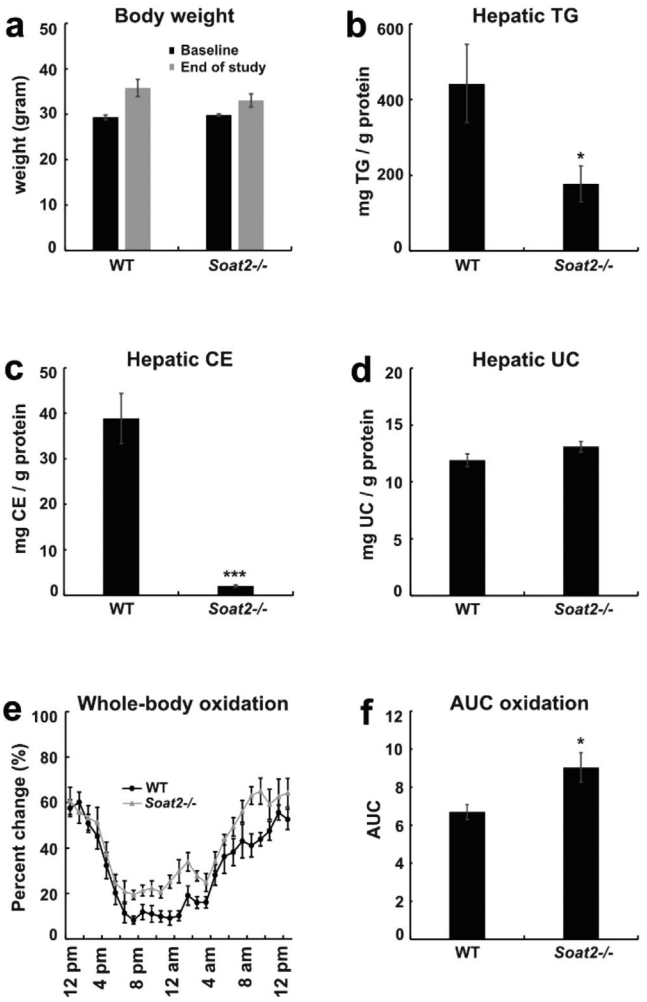

Fig. 5 *Increased whole-body oxidation in* Soat2$^{-/-}$ *mice. An additional experiment in older mice (~7 months) fed a high-fat diet for eight weeks was performed. As for younger mice, no significant differences in weight-gain (a) were observed, but hepatic lipids (b)–(d) decreased in* Soat2$^{-/-}$ *compared to wild-type (WT) mice. Metabolic studies revealed that* Soat2$^{-/-}$ *mice had about 30% higher whole-body oxidation than wild types (e and f). Data are expressed as mean ± SEM. Differences between the two genotypes were tested using the Student´s* t*-test;* *p < *0.05,* **p < *0.01, and* ***p < *0.001.*

Discussion

Our work shows for the first time that inhibition of cholesterol esterification in the liver and intestine by genetic depletion of *Soat2*, and the following lack of ACAT2 activity, lowers storage of lipids via partitioning them into oxidation pathways¸ a feature that would protect against the HFD-induced metabolic defect [17] (Fig. S6).

As *Soat2*$^{-/-}$ mice are healthy and do not present features of the metabolic syndrome, we challenged the mice with two types of diets, which have been shown in other animal models to increase hepatic and serum lipids, as well as impair glucose tolerance [25, 26]. Interestingly, in mice genetically depleted for *Soat2*, the markers of glucose tolerance (e.g. glucose, insulin, HOMA-IR, OGTT, and ITT) were strongly positively correlated to the levels of ACAT2-derived CE in the liver, which substantiates the role and relevance of *Soat2* in maintaining glucose homeostasis. The level of ACAT2-derived CE also influences the levels of TG in the liver since the positive association between the two major lipids in the liver recedes when *Soat2* is genetically depleted. Further, the presence of a strong positive correlation between the levels of TG in the liver and in serum VLDL particles only in *Soat2*$^{-/-}$ mice, and not in wild-type mice, clearly indicates that ACAT2 activity leads to a trapping of TG in the liver, in line with a previous study [12].

The relevance of our conclusions for the human condition is sustained by our observation that cholesterol-synthesis inhibition in gallstone patients leads to decreased hepatic ACAT2 activity

[27], decreased TG accumulation in the liver [28], and to decreased cholesterol remnants (non-LDL and non-HDL cholesterol) [29]. In humans, reduction of ACAT2 activity by statins was not associated with an increase in TG in VLDL particles, likely due to additional effects of cholesterol-synthesis inhibition on TG and glucose metabolism [28].

Elevated levels of TG in the circulation are a risk factor for cardiovascular events in humans. Hence, the increased TG in VLDL particles, observed in male mice genetically depleted of *Soat2*, may be interpreted as a proatherogenic lipoprotein phenotype. However, this does not seem to be the case since genetic or selective pharmacological inhibition of *Soat2* has been shown to confer protection against atherosclerosis, despite the increase in TG in circulation [7–11]. This apparently paradoxical condition can be explained by the observation that enrichment in ACAT2-derived CE increases proteoglycan binding of LDL and promotes atherosclerosis in mice [30], and is further supported by the recognition that CE in the core of TG-rich apoB-containing particles—which are mainly synthetized by ACAT2 in the intestine and in the liver—promote atherosclerosis in humans, independent of LDL cholesterol [31]. The overall result would be an increase in TG mobilization from the liver but also a synergistic shift in peripheral nutrient partitioning in favour of lipid substrate oxidation. This phenotype has also been associated with an increase in plasma TG but paradoxical improvement of glucose tolerance onto HFD [17].

Blood glucose is transported across the plasma membrane into the liver by GLUT2 and immediately phosphorylated by GCK. The expression of GLUT2 has been reported to be increased in insulin-resistant states [32–34]. SNPs in *SLC2A2* are associated with cardiovascular disease and serum cholesterol levels [35, 36], and humans with mutations in *SLC2A2*—which cause Fanconi-Bickel syndrome—have elevated plasma cholesterol levels [37]. Also, long-term hepatic *Gck* overexpression increases markers of glucose tolerance (e.g. glucose, insulin, and OGTT), and hepatic and serum lipid levels in mice [38]. Consequently, our findings of lower GLUT2 membrane protein expression and lower *Gck* mRNA levels in *Soat2*$^{-/-}$ mice further support the relevance of ACAT2/*Soat2* in maintaining glucose homeostasis.

High serum levels of glucose and insulin also inhibit fatty acid oxidation [39]. Hence, it is not surprising that ACAT2 inhibition by genetic depletion of *Soat2* induces whole-body oxidation as a likely consequence of the lower fasting insulin levels in circulation, which is paralleled by lower or unchanged glucose levels. An interesting finding is that genetic depletion of *Soat2* doubled the expression of *Cpt1a* only in tibialis anterior—which is a glycolytic muscle—whereas no increases were observed in soleus, liver, or adipose tissue (Fig. S5). This interesting finding—which suggests a switch towards a more oxidative phenotype in tibialis anterior—was paralleled by a different and inconsistent behaviour of the *Acadm* gene, which was slightly decreased in the liver, soleus, and tibialis anterior but increased by 50% in adipose tissue of *Soat2*$^{-/-}$ mice. Glucose is the main substrate for DNL, which is elevated in T2DM and NAFLD. As in female *Soat2*$^{-/-}$ mice challenged by the same diets [13], male mice depleted for *Soat2* seem to have reduced DNL—following decreased expression of *Acaca*—which in turn contributes to the reduced hepatic steatosis and improved glucose tolerance observed in *Soat2*$^{-/-}$ mice.

In adipose tissue, insulin suppresses lipolysis, promotes lipogenesis, and increases glucose uptake. Adipo-IR is considered a surrogate marker of insulin resistance in adipose tissue, and it gradually increases from a normal condition to impaired glucose tolerance and finally to overt T2DM [40]. In line with the improved glucose tolerance in *Soat2*$^{-/-}$ mice, it seems that genetic depletion of *Soat2* positively affects the insulin resistance of adipose tissue, since Adipo-IR was lower compared to wild-type mice. The mechanism behind this is yet unknown. We cannot exclude that the different composition of CE in the circulating apoB-containing lipoproteins [4] may play a role, by exposing the adipose tissue to different loads of cholesterol and CE species. Our hypothesis is also supported by the identification of a role for cholesterol, and its esterification, in lipolysis and insulin signaling of adipocytes [41]. Hence, it seems that the positive effects of *Soat2* depletion go beyond decreased hepatic lipid accumulation and improved hepatic glucose tolerance and involve the adipose tissue and the muscles, in which lower accumulation of lipids is observed.

Dysregulation of LD physiology and metabolism also increases the risk of developing T2DM and NAFLD. The expression of FSP27/CIDEC is high in adipose tissue, low in normal livers, and highly induced in fatty livers [23, 24]. A key finding of

our studies is that genetic depletion of *Soat2* either blunts (HCD) or dampens (HFD) the increase in hepatic *Fsp27/Cidec* mRNA levels. In contrast, no significant differences in *Fsp27* mRNA levels in the adipose tissue were observed between *Soat2* $^{-/-}$ and wild-type mice (data not shown). Adipocyte-specific [42] or total *Fsp27* knockout mice challenged with HFD have lower body weight and less fat mass, but this is accompanied by hepatic steatosis and insulin resistance [43]. Partial lipodystrophy and insulin-resistant diabetes have also been reported in a woman bearing a nonsense mutation in *CIDEC* [44]. It is thus clear that inhibition of FSP27/CIDEC in adipose tissue should be avoided. Interestingly, overexpression of FSP27 in mouse hepatocytes increases intracellular TG accumulation, impairs mitochondrial β-oxidation, and reduces TG turnover [45]. Here we found genetic depletion of *Soat2* to be associated with lower FSP27/CIDEC, diminished hepatic steatosis, improved glucose tolerance, and enhanced β-oxidation. Reduced hepatic *Fsp27/Cidec* levels in *Soat2*$^{-/-}$ mice seem thus to be an important mechanism by which depletion of *Soat2* results in improved hepatic steatosis and glucose tolerance.

The results in this and previous studies [7–13] contrast with the study by Wang et al. [46], which reported no significant differences in hepatic and serum TG levels between *Soat2*$^{-/-}$ and wild-type mice when fed either HFD (60% kcal% fat) or a chow diet for 12 weeks. Also, in contrast to our study, increased serum levels of NEFA, AUC GTT, and AUC ITT were reported in *Soat2*$^{-/-}$ fed HFD, but not the chow diet [46]. The *Soat2*$^{-/-}$ mice used in the study [46] are of the same origin as ours and the studies mentioned earlier. The diet and the feeding period differ, but it seems unlikely that this could explain the discrepancy. It is challenging to resolve the discrepancy in findings of this study with that of Wang et al. [46] as they did not: (a) report potential differences in body weight at baseline and weight-gain during the course of the study; (b) assess serum levels of glucose and insulin levels and calculation of HOMA-IR; (c) perform OGTT tests (i.p. injection of glucose was performed); or(d) assess glucose tolerance in various tissues (e.g. liver, adipose) and skeletal muscles. Nevertheless, the lack of significant differences in serum VLDL-TG in *Soat2*$^{-/-}$ compared to wild-type mice seems to be one of the most relevant mechanistic explanations to the discrepancies.

In conclusion, our study reveals the mechanisms by which ACAT2, encoded by *Soat2*, and ACAT2-derived CE modulate glucose and lipid metabolism, and insulin resistance (Fig. S6). It also shows how cholesterol esterification by ACAT2 affects β-oxidation and how the ACAT2-derived CE regulates the mobilization of TG from the liver. The positive effects on adipose tissue and muscles also suggest that genetic depletion of *Soat2* ameliorates the metabolic status of mice, beyond the observed diminished or complete resistance to hepatic steatosis. Our study strongly suggests specific inhibition of ACAT2 as an effective strategy to reduce liver lipid accumulation—a strategy with positive consequences beyond the cardiometabolic diseases as suggested by the recent finding that ACAT2/*SOAT2* increases the risk for NAFLD following hepatitis C virus infection [14].

Acknowledgements

The authors thank Anita Lövgren-Sandblom, Division of Clinical Chemistry, Department of Laboratory Medicine, Karolinska Institutet, Stockholm, Sweden, for invaluable technical assistance. This work was supported by grants from the Swedish Research Council, the Swedish Heart-Lung Foundation, the Stockholm City Council, Karolinska Institutet, the Swedish Old Servant Foundation, the Diabetes Foundation, and the NovoNordisk Foundation.

Author contributions

PP and CP came up with the hypotheses and designed the study. CP, OA, LL, MP, MM, SL, RD, JH, LLV, KRS, MR and LH carried out analyses. CP collated and analysed the data. OA set up the database. CP, OA and PP performed statistical analyses. CP, ME and PP drafted the manuscript, and all authors critically reviewed the manuscript. ME and PP secured funding.

Conflict of interest

The authors have no conflict of interest to declare.

References

1 Mooradian AD. Dyslipidemia in type 2 diabetes mellitus. *Nat Clin Pract.* 2009;**5**:150–9.
2 Pramfalk C, Davis MA, Eriksson M, Rudel LL, Parini P. Control of ACAT2 liver expression by HNF1. *J Lipid Res.* 2005;**46**:1868–76.
3 Pramfalk C, Karlsson E, Groop L, Rudel LL, Angelin B, Eriksson M, et al. Control of ACAT2 liver expression

by HNF4{alpha}: lesson from MODY1 patients. *Arterioscler Thromb Vasc Biol.* 2009;**29**:1235–41.
4 Pramfalk C, Eriksson M, Parini P. Cholesteryl esters and ACAT. *Eur J Lipid Sci Tech.* 2012;**114**:624–33.
5 Parini P, Davis M, Lada AT, Erickson SK, Wright TL, Gustafsson U, *et al.* ACAT2 is localized to hepatocytes and is the major cholesterol-esterifying enzyme in human liver. *Circulation.* 2004;**110**:2017–23.
6 Zhang J, Sawyer JK, Marshall SM, Kelley KL, Davis MA, Wilson MD, *et al.* Cholesterol esters (CE) derived from hepatic sterol *O*-acyltransferase 2 (SOAT2) are associated with more atherosclerosis than CE from intestinal SOAT2. *Circ Res.* 2014;**115**:826–33.
7 Willner EL, Tow B, Buhman KK, Wilson M, Sanan DA, Rudel LL, et al. Deficiency of acyl CoA:cholesterol acyltransferase 2 prevents atherosclerosis in apolipoprotein E-deficient mice. *Proc Natl Acad Sci U S A.* 2003;**100**:1262–7.
8 Buhman KK, Accad M, Novak S, Choi RS, Wong JS, Hamilton RL, *et al.* Resistance to diet-induced hypercholesterolemia and gallstone formation in ACAT2-deficient mice. *Nat Med.* 2000;**6**:1341–7.
9 Bell TA, 3rd, Brown JM, Graham MJ, Lemonidis KM, Crooke RM, Rudel LL. Liver-specific inhibition of acyl-coenzyme A:cholesterol acyltransferase 2 with antisense oligonucleotides limits atherosclerosis development in apolipoprotein B100-only low-density lipoprotein receptor$^{-/-}$ mice. *Arterioscler Thromb Vasc Biol.* 2006;**26**:1814–20.
10 Bell TA, 3rd, Kelley K, Wilson MD, Sawyer JK, Rudel LL. Dietary fat-induced alterations in atherosclerosis are abolished by ACAT2-deficiency in ApoB100 only, LDLr$^{-/-}$ mice. *Arterioscler Thromb Vasc Biol.* 2007;**27**:1396–402.
11 Ohshiro T, Matsuda D, Sakai K, Degirolamo C, Yagyu H, Rudel LL, *et al.* Pyripyropene A, an acyl-coenzyme A:cholesterol acyltransferase 2-selective inhibitor, attenuates hypercholesterolemia and atherosclerosis in murine models of hyperlipidemia. *Arterioscler Thromb Vasc Biol.* 2011;**31**:1108–15.
12 Alger HM, Brown JM, Sawyer JK, Kelley KL, Shah R, Wilson MD, et al. Inhibtion of acyl-coenzyme A:cholesterol acyltransferase 2 (ACAT2) prevents dietary cholesterol associated steatosis by enhancing hepatic triglyceride mobilization. *J Biol Chem.* 2010;**285**:14267–74.
13 Ahmed O, Pramfalk C, Pedrelli M, Olin M, Steffensen KR, Eriksson M, et al. Genetic depletion of Soat2 diminishes hepatic steatosis via genes regulating de novo lipogenesis and by GLUT2 protein in female mice. *Dig Liv Dis.* 2019;**51**:1016–22.
14 Sun HY, Chen TY, Tan YC, Wang CH, Young KC. Sterol *O*-acyltransferase 2 chaperoned by apolipoprotein J facilitates hepatic lipid accumulation following viral and nutrient stresses. *Commun Biol.* 2021;**4**:564.
15 Pedrelli M, Davoodpour P, Degirolamo C, Gomaraschi M, Graham M, Ossoli A, et al. Hepatic ACAT2 knock down increases ABCA1 and modifies HDL metabolism in mice. *PLoS One.* 2014;**9**:e93552.
16 Parini P, Johansson L, Broijersen A, Angelin B, Rudling M. Lipoprotein profiles in plasma and interstitial fluid analyzed with an automated gel-filtration system. *Eur J Clin Invest.* 2006;**36**:98–104.
17 Joly-Amado A, Denis RGP, Castel J, Lacombe A, Cansell C, Rouch C, et al. Hypothalamic AgRP-neurons control peripheral substrate utilization and nutrient partitioning. *EMBO J.* 2012;**31**:4276–88.
18 Hodson L, Bickerton AS, McQuaid SE, Roberts R, Karpe F, Frayn KN, et al. The contribution of splanchnic fat to VLDL triglyceride is greater in insulin-resistant than insulin-sensitive men and women: studies in the postprandial state. *Diabetes.* 2007;**56**:2433–41.
19 Barrows BR, Parks EJ. Contributions of different fatty acid sources to very low-density lipoprotein-triacylglycerol in the fasted and fed states. *J Clin Endocrinol Metab.* 2006;**91**:1446–52.
20 Lewis GF, Uffelman KD, Szeto LW, Weller B, Steiner G. Interaction between free fatty acids and insulin in the acute control of very low density lipoprotein production in humans. *J Clin Invest.* 1995;**95**:158–66.
21 Picard F, Boivin A, Lalonde J, Deshaies Y. Resistance of adipose tissue lipoprotein lipase to insulin action in rats fed an obesity-promoting diet. *Am J Physiol.* 2002;**282**:E412–8.
22 Lawrence JC, Gower BA, Timothy Garvey W, Julian Munoz A, Darnell BE, Oster RA, et al. Relationship between insulin sensitivity and muscle lipids may differ with muscle group and ethnicity. *Open Obes J.* 2010;**2**:137–44.
23 Matsusue K, Kusakabe T, Noguchi T, Takiguchi S, Suzuki T, Yamano S, et al. Hepatic steatosis in leptin-deficient mice is promoted by the PPARgamma target gene Fsp27. *Cell Metab.* 2008;**7**:302–11.
24 Toh SY, Gong J, Du G, Li JZ, Yang S, Ye J, et al. Up-regulation of mitochondrial activity and acquirement of brown adipose tissue-like property in the white adipose tissue of fsp27 deficient mice. *PLoS One.* 2008;**3**:e2890.
25 Korach-Andre M, Archer A, Gabbi C, Barros RP, Pedrelli M, Steffensen KR, *et al.* Liver X receptors regulate de novo lipogenesis in a tissue-specific manner in C57BL/6 female mice. *Am J Physiol Endocrinol Metab.* 2011;**301**:E210–22.
26 Korach-Andre M, Parini P, Larsson L, Arner A, Steffensen KR, Gustafsson JA. Separate and overlapping metabolic functions of LXRalpha and LXRbeta in C57Bl/6 female mice. *Am J Physiol Endocrinol Metab.* 2010;**298**:E167–78.
27 Parini P, Gustafsson U, Davis MA, Larsson L, Einarsson C, Wilson M, et al. Cholesterol synthesis inhibition elicits an integrated molecular response in human livers including decreased ACAT2. *Arterioscler Thromb Vasc Biol.* 2008;**28**:1200–6.
28 Pramfalk C, Parini P, Gustafsson U, Sahlin S, Eriksson M. Effects of high-dose statin on the human hepatic expression of genes involved in carbohydrate and triglyceride metabolism. *J Intern Med.* 2011;**269**:333–9.
29 Ahmed O, Littmann K, Gustafsson U, Pramfalk C, Öörni K, Larsson L, et al. Ezetimibe in combination with simvastatin reduces remnant cholesterol without affecting biliary lipid concentrations in gallstone patients. *J Am Heart Assoc.* 2018;**7**:e009876.
30 Melchior JT, Sawyer JK, Kelley KL, Shah R, Wilson MD, Hantgan RR, et al. LDL particle core enrichment in cholesteryl oleate increases proteoglycan binding and promotes atherosclerosis. *J Lipid Res.* 2013;**54**:2495–503.
31 Nordestgaard BG. Triglyceride-rich lipoproteins and atherosclerotic cardiovascular disease: new insights from epidemiology, genetics, and biology. *Circ Res.* 2016;**118**:547–63.
32 Marks J, Carvou NJ, Debnam ES, Srai SK, Unwin RJ. Diabetes increases facilitative glucose uptake and GLUT2 expression at the rat proximal tubule brush border membrane. *J Physiol.* 2003;**553**:137–45.

33 Narasimhan A, Chinnaiyan M, Karundevi B. Ferulic acid regulates hepatic GLUT2 gene expression in high fat and fructose-induced type-2 diabetic adult male rat. *Eur J Pharmacol.* 2015;**761**:391–7.
34 Im SS, Kang SY, Kim SY, Kim HI, Kim JW, Kim KS, et al. Glucose-stimulated upregulation of GLUT2 gene is mediated by sterol response element-binding protein-1c in the hepatocytes. *Diabetes.* 2005;**54**:1684–91.
35 Borglykke A, Grarup N, Sparsø T, Linneberg A, Fenger M, Jeppesen J, et al. Genetic variant SLC2A2 [corrected] is associated with risk of cardiovascular disease—assessing the individual and cumulative effect of 46 type 2 diabetes related genetic variants. *PLoS One.* 2012;**7**: e50418.
36 Igl W, Johansson A, Wilson JF, Wild SH, Polašek O, Hayward C, *et al.* Modeling of environmental effects in genome-wide association studies identifies SLC2A2 and HP as novel loci influencing serum cholesterol levels. *PLoS Genet.* 2010;**6**:e1000798.
37 Taha D, Al-Harbi N, Al-Sabban E. Hyperglycemia and hypoinsulinemia in patients with Fanconi-Bickel syndrome. *J Pediatr Endocrinol Metab.* 2008;**21**:581–6.
38 Ferre T, Riu E, Franckhauser S, Agudo J, Bosch F. Long-term overexpression of glucokinase in the liver of transgenic mice leads to insulin resistance. *Diabetologia.* 2003;**46**: 1662–8.
39 Randle PJ. Regulatory interactions between lipids and carbohydrates: the glucose fatty acid cycle after 35 years. *Diabetes Metab Rev.* 1998;**14**:263–83.
40 Kim JY, Bacha F, Tfayli H, Michaliszyn SF, Yousuf S, Arslanian S. Adipose tissue insulin resistance in youth on the spectrum from normal weight to obese and from normal glucose tolerance to impaired glucose tolerance to type 2 diabetes. *Diabetes Care.* 2019;**42**:265–72.
41 Xu Y, Du X, Turner N, Brown AJ, Yang H. Enhanced acyl-CoA:cholesterol acyltransferase activity increases cholesterol levels on the lipid droplet surface and impairs adipocyte function. *J Biol Chem.* 2019;**294**:19306–21.
42 Tanaka N, Takahashi S, Matsubara T, Jiang C, Sakamoto W, Chanturiya T, et al. Adipocyte-specific disruption of fat-specific protein 27 causes hepatosteatosis and insulin resistance in high-fat diet-fed mice. *J Biol Chem.* 2015;**290**:3092–3105.
43 Zhou L, Park S-Y, Xu L, Xia X, Ye J, Su L, et al. Insulin resistance and white adipose tissue inflammation are uncoupled in energetically challenged Fsp27-deficient mice. *Nat Commun.* 2015:**6**: 5949.
44 Rubio-Cabezas O, Puri V, Murano I, Saudek V, Semple RK, Dash S, et al. Partial lipodystrophy and insulin resistant diabetes in a patient with a homozygous nonsense mutation in CIDEC. *EMBO Mol Med.* 2009;**1**:280–7.
45 Matsusue K, Kusakabe T, Noguchi T, Takiguchi S, Suzuki T, Yamano S, et al. Hepatic steatosis in leptin-deficient mice is promoted by the PPARgamma target gene Fsp27. *Cell Metab.* 2008;**7**:302–11.
46 Wang Y-J, Bian Y, Luo J, Lu M, Xiong Y, Guo S-Y, et al. Cholesterol and fatty acids regulate cysteine ubiquitylation of ACAT2 through competitive oxidation. *Nat Cell Biol.* 2017;**19**:808–19.

Correspondence: Paolo Parini, Division of Clinical Chemistry, Department of Laboratory Medicine, Karolinska Institutet, ANA Futura, Alfred Nobels allé 8, SE-141 52 Huddinge, Sweden.
Email: paolo.parini@ki.se

Supporting Information

Additional Supporting Information may be found in the online version of this article:

Supporting Information ■